System design for a solar powered electric vehicle charging station for workplaces

Chandra Mouli, GR; Bauer, Pavol; Zeman, Miro

DOI
10.1016/j.apenergy.2016.01.110

Publication date
2016

Document Version
Final published version

Published in
Applied Energy

Applied Energy 168 (2016) 434–443

Contents lists available at ScienceDirect

Applied Energy

journal homepage: www.elsevier.com/locate/apenergy

System design for a solar powered electric vehicle charging station for workplaces ☆

G.R. Chandra Mouli, P. Bauer *, M. Zeman

Department of Electrical Sustainable Energy, Delft University of Technology, Mekelweg 4, 2628 CD Delft, The Netherlands

HIGHLIGHTS

- 10 kW solar powered EV charger with V2G for workplaces in Netherlands is analyzed.
- Optimal tilt for PV panels to get maximum yield in Netherlands is 28°.
- PV array can be 30% oversized than converter, resulting in only 3.2% energy loss.
- Gaussian EV charging profile with low peak closely follows PV generation.
- 10 kW h local storage reduced grid energy exchange by 25%.

ARTICLE INFO

Article history:
Received 18 September 2015
Received in revised form 19 January 2016
Accepted 28 January 2016
Available online 11 February 2016

Keywords:
Batteries
Electric vehicles
Energy storage
Photovoltaic systems
Solar energy

ABSTRACT

This paper investigates the possibility of charging battery electric vehicles at workplace in Netherlands using solar energy. Data from the Dutch Meteorological Institute is used to determine the optimal orientation of PV panels for maximum energy yield in the Netherlands. The seasonal and diurnal variation in solar insolation is analyzed to determine the energy availability for EV charging and the necessity for grid connection. Due to relatively low solar insolation in Netherlands, it has been determined that the power rating of the PV array can be oversized by 30% with respect to power rating of the converter. Various dynamic EV charging profiles are compared with an aim to minimize the grid dependency and to maximize the usage of solar power to directly charge the EV. Two scenarios are considered – one where the EVs have to be charged only on weekdays and the second case where EV have to be charged all 7 days/week. A priority mechanism is proposed to facilitate the charging of multiple EV from a single EV–PV charger. The feasibility of integrating a local storage to the EV–PV charger to make it grid independent is evaluated. The optimal storage size that reduces the grid dependency by 25% is evaluated.

1. Introduction

Two major trends in energy usage that are expected for future smart grids are:

1. Large-scale decentralized renewable energy production through photovoltaic (PV) system.
2. Emergence of battery electric vehicles (EV) as the future mode of transport.

Firstly, the use of renewable energy sources such as solar energy is accessible to a wider audience because of the falling cost of PV panels [1]. Industrial sites and office buildings in the Netherlands harbor a great potential for photovoltaic (PV) panels with their large surface on flat roofs. Examples include warehouses, industrial buildings, universities, factories, etc. This potential is largely unexploited today. Secondly, EVs provide a clean, energy efficient and noise-free means for commuting when compared with gasoline vehicles. The current forecast is that in the Netherlands there will be 200,000 EV in 2020 [2].

This paper examines the possibility of creating an electric vehicle charging infrastructure using PV panels as shown in Fig. 1. The system is designed for use in workplaces to charge electric cars of the employees as they are parked during the day. The motive is to maximize the use of PV energy for EV charging with minimal energy exchange with the grid. The advantages of such an EV–PV charger will be:

☆ This work was supported by TKI Switch2SmartGrids Grant, Netherlands.
* Corresponding author at: Faculty of EEMCS (Building 36), Delft University of Technology, Mekelweg 4, 2628 CD Delft, The Netherlands. Tel.: +31 (0)15 27 84654.
E-mail addresses: G.R.Chandamouli@tudelft.nl (G.R. Chandra Mouli), P.Bauer@tudelft.nl (P. Bauer), M.Zeman@tudelft.nl (M. Zeman).

http://dx.doi.org/10.1016/j.apenergy.2016.01.110
0306-2619/

Fig. 1. Design of solar powered EV charging station.

1. Reduced energy demand on the grid due to EV charging as the charging power is locally generated in a 'green' manner through solar panels.
2. EV battery doubles up as an energy storage for the PV and reduces negative impact of large scale PV integration in distribution network [3].
3. Long parking time of EV paves way for implementation of Vehicle-to-grid (V2G) technology where the EV acts as a controllable spinning reserve for the smart grid [4–7].

Several earlier works have analyzed the design of an EV charging station based on PV [8–17]. The mutual benefit of charging EV from solar energy has been highlighted in [18,19] where the potential to charge EV from solar allows for higher penetration of both technologies. In [20], the negative effects of excess solar generation from PV on a national level has been shown to be mitigated by using it for charging EVs. This is especially applicable for charging at workplace as shown in [19]. In [21,22], for the case of Columbus and Los Angeles, USA, the economic incentive and CO_2 offsets for PV charging have been shown to be greater than charging the EV from grid.

A major disadvantage of charging EV from PV is the variability in the PV production. Smart charging provides for flexibility of EV charging in order to closely match the PV production. [23] has shown that smart charging combined with V2G has the dual benefit of increasing PV self-consumption and reducing peak demand on grid. In [24], the EV charging profile is varied with time so that maximum PV utilization occurs. In can be seen that the excess PV energy reduces with higher EV penetration [25,26]. Alternately, the total number of vehicles that are charging at a constant power can be dynamically varied so that the net charging power follows the PV generation, as seen in [27]. This type of sequential charging shows great benefit than simultaneous EV charging, which is proved in [28] by considering 9000 different cases. A time shift scheduling is used in [29] to manage the charging of e-scooters so that the net charging power follows the PV profile. This method is further improved with the use of weather forecast data [30].

A second method to overcome the PV variation is to use a local storage in the PV powered EV charging station, like in [26,31–35]. The storage is typically charged when there is excess solar energy and is then used to charge the EV when solar generation is insufficient [26]. In [36], three different algorithms for (dis)charging the local storage are compared and it was shown that a sigmoid function based discharging of the storage and charging during night and solar excess was the best strategy.

Since storage is an expensive component, optimally sizing the storage is vital. This aspect has been neglected by the papers mentioned above. Secondly, research works that analyzed the use of smart charging have not considered the use of local storage and vice versa. The two methods are investigated together in this work for a solar powered EV charging station. Thirdly, in case of workplace charging it is important to distinguish the effects of weekday and weekend EV charging load. This is because rooftop PV installed in workplace will produce energy even in the weekends even though the EVs of the employee are not present on Saturday-Sunday. This paper analyses the PV system design and EV charging in a holistic manner considering the above aspects. The new contributions of the work compared to earlier works are as follows:

1. Determination of the optimal orientation of PV panels for maximizing energy yield in Netherlands and comparing it with the use of tracking systems.
2. Possibility of oversizing the PV array power rating with respect to the power converter size based on metrological conditions of the location.
3. Dynamic charging of EV using Gaussian charging profile and EV prioritization, which is superior to constant power charging.
4. Determination of grid impact of two different types of workplace/commercial charging scenario considering 5 days/week and 7 days/week EV load by running round-the-year simulation.
5. Optimal sizing of local storage considering both meteorological data and smart charging of EV

The paper is divided into five sections. In the second section, a model is developed to estimate the electricity output of a PV system in the Netherlands, taking into account the meteorological conditions. The optimal orientation of PV panels in the Netherlands for maximum yield is determined. In the third section, different dynamic charging strategies for EV are analyzed, such that EV charging can closely follow the PV generation. In the fourth section, the benefits of having local battery storage in the EV–PV charger are investigated and the optimal storage size is determined.

2. EV charging in workplace using PV

EV charging in Europe is defined by the standards in [37,38]. The charging plug type widely used in Europe for AC charging is the Type 2 Mennekes plug. It supports both single and three phase AC charging at Level 2 charging power level [39].

However in the future, DC charging using Chademo and the Combined Charging Standard (CCS) will be most preferred charging standard for charging EV from PV at workplace due to the following reasons:

1. Both EV and PV are inherently DC by nature.
2. Dynamic charging of EV is possible, where the EV charging power can be varied with time.
3. DC charging facilitates vehicle-to-grid (V2G) protocol.

In this paper, a 10 kW EV–PV charger will be considered that provides both charging and discharging of car for up to 10 kW, as shown in Fig. 2. This is in line with the draft proposal of the Chademo standard for enabling 10 kW V2G from EV. The three-port converter connected to the 50 Hz AC grid was chosen as the most suitable system architecture based on [12]. Since the cars are parked for long durations of 7–9 h at the workplace, fast charging of EV at 50 kW or more would be unnecessary. Solar power is the primary power source of the grid connected EV–PV charging system. The solar power is generated using a 10 kW_p photovoltaic (PV) array that is located at the workplace. The panels could be located on the roof top of the buildings or installed as a solar carport [8].

The EV–PV charger has two bidirectional ports for the grid and EV, and one unidirectional port for PV. The PV converter, grid

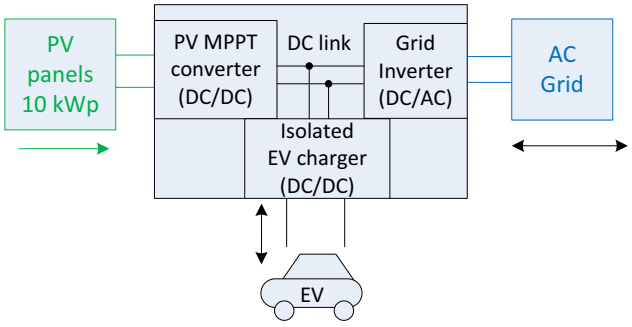

Fig. 2. System architecture of the grid connected 10 kW three-port EV–PV charger.

inverter and the isolated EV charger are integrated on a central DC-link. Direct interfacing of EV and PV on DC would be more beneficial than AC interfacing due to lower conversion steps and improved efficiency [10,12,40,41].

3. PV system design

3.1. Estimation of optimal orientation of PV array in the Netherlands

To evaluate the power and energy generated by a 10 kW_p PV array in the Netherlands, an accurate measurement of weather data is required. For this purpose, the meteorological data from the Dutch Meteorological Institute (KNMI) is used, which has a resolution of 1 min [42]. Global horizontal irradiance (S^{GHI}), Diffuse Horizontal Irradiance (S^{DHI}), Direct Normal Irradiance (S^{DNI}) and ambient temperature (T_a) are obtained from KNMI for the years 2011–2013. A 10 kW_p PV array was modelled in MATLAB using 30 modules of Sun power E20-327 modules rated at 327 W [43], whose specifications are shown in Table 1. They are connected in 5 parallel strings having 6 modules in series having a combined installed power of 9810 W.

To estimate the solar irradiance on a module (S_m) with a specific azimuth (A_m) and tilt angle (θ_m) as shown in Fig. 3, an estimation of the position of the sun throughout the year is required. A solar position calculator is hence built using [44,45] by which the azimuth (A_s) and altitude (a_s) of the sun throughout the year at the location of the KNMI observatory can be determined. With the sun's position, the irradiance on a panel with specific orientation (A_m, θ_m) can be estimated using the geometric models in [46–48] and the Isotropic sky diffused model [46,49] where $S^{DNI}{}_m$, $S^{DHI}{}_m$ are the components of DNI and DHI which is incident on the panel:

$$S_m^{DNI} = S^{DNI}(\sin\theta_m \cos a_s \cos(A_m - A_s) + \cos\theta_m \sin a_s) \quad (1)$$

$$S_m^{DHI} = S^{DHI}\frac{1+\cos\theta_m}{2} \quad (2)$$

$$S_m = S_m^{DHI} + S_m^{DNI} \quad (3)$$

Table 1
Parameters of Sun power E20-327 module.

Quantity	Value
Area of module (A_{pv})	1.63 m^2
Nominal power (P_r)	327 W
Avg. panel efficiency (η)	20.4%
Rated voltage (V_{mpp})	54.7 V
Rated current (I_{mpp})	5.98 A
Open-circuit voltage (V_{oc})	64.9 V
Short-circuit current (I_{sc})	6.46 A
Nominal operating cell temperature (T_{NOCT})	45 °C ± 2 °C
Power temp coefficient (λ)	−0.38%/°C

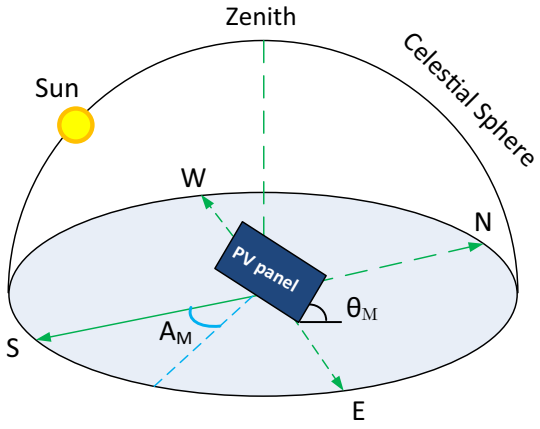

Fig. 3. Orientation of the PV panel is defined by azimuth angle A_m (measured from the South) and module tilt angle θ_m (measured from horizontal surface).

In order estimate the output power of a PV array, it is important to consider the ambient temperature, besides the magnitude of incident solar insolation. The PV array is rated for 327 W at the STC ambient temperature of 25°. For other ambient temperatures (T_a), the PV array output power (P_m) can be estimated using [50–52], where T_{cell} is the temperature of the PV cells:

$$T_{cell} = T_a + \frac{S_m}{800}(T_{NOCT} - 20) \quad (4)$$

$$P_m = \frac{P_r S_m}{1000}[1 - \lambda(T_{cell} - 25)] \quad (5)$$

Using the above equations and meteorological data from KNMI, the output of the 10 kW PV array can be estimated. For geographical locations in the northern hemisphere like Netherlands, the optimal azimuth for the PV panels is $A_m = 0°$ i.e. facing south. To determine the optimal tilt angle θ_m, the annual energy yield of the 10 kW PV system is determined for different tilt angles, as shown in Fig. 4.

It can be observed that for an optimal tilt of 28°, maximum annual energy yield is obtained for the years 2011-13, with an average value of 10,890 kW h. The corresponding average daily yield for the PV system is 29.84 kW h/day. It must be kept in mind that in practice, it might not be possible to install the PV panels along the optimal orientation due to characteristics of the roof [48]. Further, shading on the panels due to nearby buildings, trees and/or other objects will reduce the yield of the PV system [52]. Since the orientation and shading will vary on a case-to-case basis, the detailed analysis of both is beyond the scope of this research work.

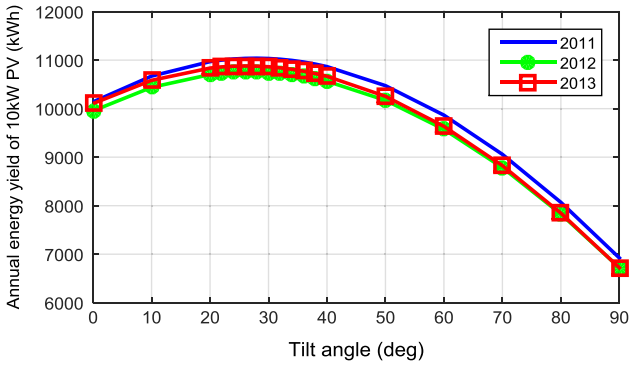

Fig. 4. Annual energy yield of 10 kW PV system as a function module tilt for years 2011-13. The PV modules were oriented south with azimuth of 0°.

3.2. Estimation of power output of optimally orinetated PV array in the Netherlands

Using an optimally oriented PV array with $A_m = 0°$ and $\theta_m = 28°$, the power production over one year is estimated using Eqs. (1)–(5) and is shown in Figs. 5 and 6. In Fig. 5., the output power of the 10 kW array for every minute can be seen over the year. The seasonal variation in peak output power over one year can be perceived, the highest being close to 12 kW in May. However, the peak power output in the winter months of November to January is only 4 kW. When the yearly data estimated in Fig.5 is averaged over a 24 h period for each month, we get the average 24 h PV profile for different months of 2013 as shown in Fig. 6. Two vital observations are:

1. The average monthly peak power ranges between 7 kW in July and 2 kW in November. This indicates that the PV system on an average only produces 70% of its rated power even in the sunniest month of the year.
2. PV generation is restricted to only 7–8 h in the winter months while it is 15 h in summer.

Figs. 7 and 8 show the daily yield of the PV system for each day of the year and as a monthly average for 2013. They clearly show the seasonal variation in PV yield. The actual yield has a variation between 75 kW h/day and 1 kW h/day for specific days in June and December respectively. With respect to the average daily yield for different months, a difference of up to 5 times can be observed between summer and winter in Fig. 8. It can also be observed that even in summer, there are cloudy days with low daily yield of <10 kW h and sunny days in winter with yield >20 kW h.

The daily yield values are compared with the 24 kW h battery pack of the Nissan Leaf EV in Figs. 7 and 8. For 54% of the year, the daily yield is greater than 24 kW h/day and for 22% of the year, the yield is greater than 48 kW h/day which equals the combined capacity of two Nissan Leafs. Thus there is a huge difference in energy availability between different days of the year. This seasonal difference in generation directly necessitates the need for a grid connected PV system that can ensure reliable power supply to the EV battery throughout the year.

Since the bottleneck in the PV system design is the low winter yield which is of the order of 10 kW h/day, the applicability of a sun tracking system to improve winter yield was investigated. The simulations were performed considering the panels to be mounted on a 2-axis tracker ($A_m = A_s$, $\theta_m = 90\text{-}a_s$) and a 1-axis tracker with either tracking of the sun's azimuth ($A_m = A_s$) or the sun's altitude ($\theta_m = 90\text{-}a_s$).

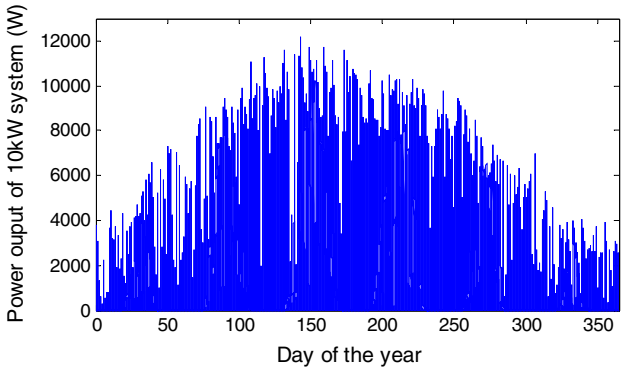

Fig. 5. Power output of 10 kW PV system as a function of time for 2013. The PV modules were oriented south with a tile angle of 28°.

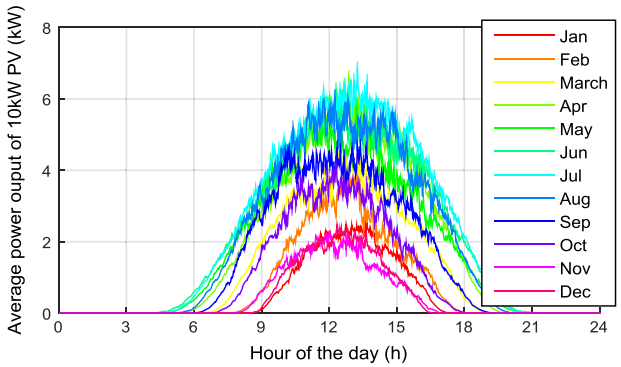

Fig. 6. Average power output of 10 kW PV system as a function of time of the day for different months of 2013.

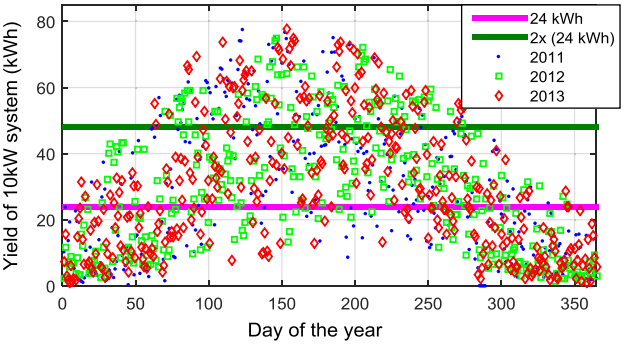

Fig. 7. Daily energy yield of 10 kW PV system for different days of 2013.

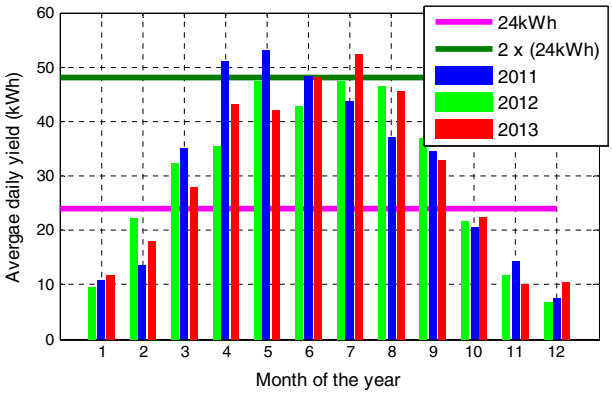

Fig. 8. Average daily yield for 10 kW PV system for different months of 2013.

The average daily yield and the annual yield due to use of a tracking system is shown in Fig. 9 and Table 2 respectively. Compared to fixed orientation of $\theta_m = 28°$ $A_m = 0°$, 17.3% and 13.3% improvement in annual yield is obtained using the 2-axis and 1-axis azimuth tracking system respectively. The 1-axis altitude tracker however results in 7.5% reduction in yield. Average gain in yield in the winter months of November to February due to a 2-axis tracker is 1.9 kW h/day while in summer the gain is as high as 11.6 kW h/day for month of July. The concentrated gains in summer make the use of tracking system unattractive in improving the winter PV yield. Further, the tracking system is economically infeasible as the 160€ or 208€ gain in energy cost/year as seen in Table 2 cannot offset the 4750€ or 8177€ cost of installing a single or dual axis tracking system respectively (Based on [53], 0.57$/W and 0.98 $/W is cost for 1-axis and 2-axis tracking system and 1.2$ = 1€).

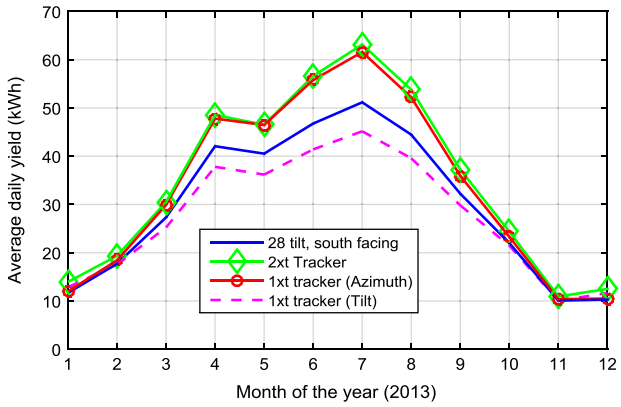

Fig. 9. Variation of the average monthly yield for 2013 for fixed orientation and when single/dual axis tracking system is used.

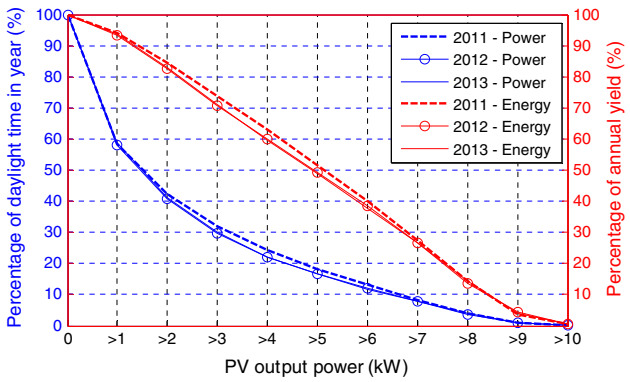

Fig. 10. Frequency distribution of output power of PV system shown as a percentage of daylight time (when PV power output is non-zero) and distribution of annual yield shown as a function of output power.

3.3. Oversizing the PV array power rating with respect to PV converter power rating

Fig. 10 and Table 3 show the frequency distribution of the PV output power as a percentage of the daylight time of the year and the corresponding energy distribution. The daylight time corresponds to the total sum of hours in the year when the PV output power is non-zero, which is 4614.5 h in 2013. While the occurrence of high output power from PV panels is low, the energy delivered by the panels at times of high output power is very high. PV Power >5 kW occur only 16% of the daylight time but delivers about 50% of annual PV energy.

Similarly PV power >7 kW and >8 kW deliver 26% and 14% of annual energy respectively as elaborated in Table 3. From the table, we can infer that by under-sizing the PV power converter by a factor of 0.9, we will lose only 0.16% of the annual energy yield. This is because, during times the PV panels can produce >9 kW, the inverter will not shut down, it will just produce 9 kW. Similarly, using a converter of 70% or 50% of the PV rated power results in only loss of 3.2% or 13.8% of annual yield as shown in Table 4. This observation opens up the opportunity for the PV panel to be oversized compared to the power converter rating in a country like Netherlands.

4. Dynamic charging of EV

Dynamic charging refers to charging the EV at variable charging power instead of a fixed power. The motive of dynamic smart charging of the EV is to vary the EV charging power to closely follow the PV generation, so that minimum power is fed/drawn from the grid.

The power drawn or fed to the grid can be expressed as given below where P_{PV}, P_{EV} are the PV generation and the EV charging power respectively:

$$P_{grid} = P_{EV} - P_{PV} \quad (6)$$

Table 3
Energy delivered and occurrence of different PV output power.

	PV power output (kW)			
	>2 kW	>5 kW	>7 kW	>9 kW
% Daylight time	41.3	16.5	7.7	0.95
% Annual energy	82.7	48.8	26	3.8

Table 4
Reduction in annual PV yield due to oversizing of PV array compared to PV converter.

	Inverter size for 10 kW PV array			
	2 kW	5 kW	7 kW	9 kW
% Energy lost in year	47.5	13.84	3.2	0.16

When $P_{grid} > 0$, power is drawn from the grid while power is fed to the grid when $P_{grid} < 0$. It is assumed that all the EVs arrive at the workplace at 0830 h and are parked till 1700 h, for a total duration of 8.5 h. 8 different EV charging profiles are compared and they are shown in Fig. 11 along with the average PV generation profile for different months. The charging profiles here are categorized into three types – Gaussian (G1, G2, G3, and G4), fixed (F1, F2) and rectangular profiles (R1, R2) based on the shape of the 24-h EV power-time curve, as shown in Fig. 11 and explained in Table 5. The fixed and rectangular charging profiles are chosen as they correspond to current EV chargers available in the market than can charge the car with a fixed time in-varying charging power. The Gaussian charging profiles were chosen due to their ability to closely match solar irradiance data [54,55] and they have their peaks at 1200 h when the sun is at its peak.

The energy delivered by each charging profile E_{PV} can be determined by integrating the power-time curve to obtain the area under the curve:

Table 2
Annual energy yield of PV system with 28° tilt and 2-axis tracker.

	Annual energy yield (kW h)				Gain/loss in energy yield (%)	Economic gain/loss [a] (€)
	2011	2012	2013	Average		
28° tilt	11039.7	10753.5	10876.2	10,890	–	–
2 axis tracker	13,114	12,483	12,732	12,776	17.3	207.5
1 axis tracker (Azimuth)	12,573	12,116	12,329	12,339	13.3	159.4
1 axis tracker (Tilt)	10,255	9946	10,022	10,074	−7.5	−89.7

[a] Based on industrial electricity price of 0.11 €/kW h.

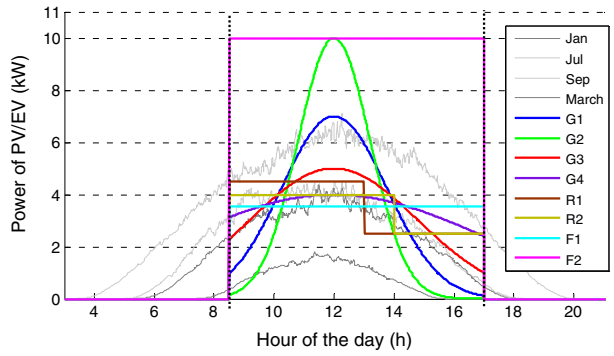

Fig. 11. Various EV charging profiles compared with the average daily PV array output for different months of 2013.

Table 5
Maximum power and energy of the 8 EV charging profiles.

EV Charging profile	Max. charging power (kW)	Energy delivered to EV (kW h)
G1 – Gaussian profile	10	30
G2 – Gaussian profile	7	30
G3 – Gaussian profile	5	30
G4 – Gaussian profile	4	30
R1 – Rectangular (4.5 kW, 2.44 kW)	4.5	30
R2 – Rectangular (4 kW, 2.67 kW)	4	30
F1 – Constant power (2.58 kW)	2.58	30
F2 – Constant power (10 kW)	10	85

$$E_{PV} = \int_{t=0830\ h}^{t=1700\ h} P_{EV}(t)dt \tag{7}$$

All charging profiles deliver 30 kW h/day to the EV battery except profile F2 which delivers 85 kW h. If a daily commuting distance of 50 km/day is considered based on [56], 10 kW h/day charging energy is required by a Nissan Leaf (121 km range as per EPA driving cycle) assuming 95% charging efficiency. 30 kW h/day thus corresponds to the commuting energy needs of three EVs. It also equals the average daily energy yield of the 10 kW PV system as per Table 2.

4.1. Matching the dynamic charging of EV to PV generation

Due to seasonal and diurnal variation in solar generation, there will always be a mismatch between EV demand and PV generation. This difference in power is fed/drawn from the grid. The total energy fed to the grid E^{grid}_{fed} and drawn from the grid E^{grid}_{draw} over one year (8760 h) can be estimated as:

$$\text{If } P_{grid}(t) < 0, E^{grid}_{fed} = \int_{t=0\ h}^{t=8760\ h} P_{grid}(t)dt \tag{8}$$

$$\text{If } P_{grid}(t) > 0, E^{grid}_{draw} = \int_{t=0\ h}^{t=8760\ h} P_{grid}(t)dt \tag{9}$$

$$E^{grid}_{ex} = E^{grid}_{draw} + |E^{grid}_{fed}| \tag{10}$$

To ensure maximum utilization of PV energy for EV charging, the total energy exchanged with the grid E^{grid}_{ex} must be minimum, assuming there is no PV power curtailment. E^{grid}_{ex} is estimated for two cases – one considering that EV is present on all 7 days of the week and the second considering that EV is present only on weekdays i.e. 5 days/week. The first case is applicable for shopping malls, theatres etc. while the second case is suitable for offices, universities and factories.

4.1.1. Scenario 1 – EV load for 7days/week

The annual PV yield for 2013 is 10,876 kW h while the annual EV demand is 10,950 kW h (30 kW h ∗ 365 days) for all profiles except F2. Table 6 shows the annual energy exchanged with the grid for different charging profiles, ranked in the order of increasing magnitude of grid energy exchange. It can be seen that annual grid energy exchange of G3, G4 is the lowest while the F2 profile results in the maximum energy exchange with the grid.

It can be observed that there exists a minimum energy that is always drawn from the grid irrespective of the charging profile. This is because while the EV demand is constant at 30 kW h throughout the year, the PV yield in winter and on cloudy days throughout the year is much less than 30 kW h, forcing the system to draw energy from the grid.

Further there is always a minimum surplus energy fed to the grid and this due to two reasons. Firstly, the peak PV array power in summer is more than the peak power of all the load profiles except G2 and F2. Secondly, the sun shines in summer months for over 16 h (0400–2000 h approx.) which is much more than the 8.5 h for which the EV is charging. This results in power being fed back to grid in the early morning and late evening.

EV charging profiles with high peak charging profiles namely G1, G2 and F2 have the lowest rank in Table 6. G3, G4, R1, R2 exhibit the better matching with PV and have a peak charging power which is the range of 40–50% of the installed watt peak of the PV array. Since lower charging power means lower component ratings in converter, it can be concluded that profile G4 with a peak EV charging power of 40% of nominal PV power, is most ideal for Netherlands.

4.1.2. Scenario 2 – EV load for 5 days/week

Simulations from scenario 1 are repeated considering the EV load to present for only 5 days/week on weekdays and no EV loads for the weekend. Only the charging profiles with rank 1–5 are considered here namely G1, G2, G3, F1, and F2. Table 7 shows the annual energy exchange with grid for different charging profiles and it can be seen that the Gaussian profiles G3, G4 exhibit minimum energy exchange. An obvious difference between the values in Tables 6 and 7 is that the energy fed to the grid has increased

Table 6
Energy exchanged with grid for 7 days/week EV load.

EV charging profile	Annual energy exchange with grid (kW h)			Rank
	Fed to grid $\lvert E^{grid}_{fed}\rvert$	Draw from grid E^{grid}_{draw}	Total E^{grid}_{ex}	
G1	5248	5350	10,598	7
G2	4455	4544	8999	6
G3	4113	4213	8326	1
G4	4119	4214	8333	2
R1	4297	4402	8699	5
R2	4180	4282	8462	3
F1	4198	4295	8493	4
F2	1336	21,546	22,882	8

Table 7
Energy exchanged with grid for 5 days/week EV load.

EV charging profile	Annual energy exchange with grid (kW h)			Rank
	Fed to grid $\lvert E^{grid}_{fed}\rvert$	Draw from grid E^{grid}_{draw}	Total E^{grid}_{ex}	
G3	6053	3024	9077	1
G4	6059	3027	9086	2
R1	6165	3141	9306	5
R2	6094	3067	9161	3
F1	6117	3088	9205	4

and the energy drawn from the grid has reduced, effectively resulting in the total energy exchanged with the grid to increase.

Fig. 13 shows the cumulated daily PV energy yield and energy fed/drawn from the grid for the year 2013 for EV load profile G4. Red circles indicate examples when the PV energy is fully fed to the grid on weekends as there is no EV load. In spite of optimal matching of the EV charging with the PV generation, surplus energy can be observed in summer months being fed to the grid and energy drawn from the grid in the winter months.

4.2. Charging of multiple EV

The Gaussian load profile G4 can deliver 30 kW h energy to EV. This energy could be distributed amongst multiple EV if each car requires less than 30 kW h of energy. Fig. 12 shows an example of the charging of three cars A, B, C with respect to the average irradiance for the month of July 2013.

Multiple cars can be arranged within the charging region and charging can be started according to priority P where B is the capacity of EV battery pack (kW h); t_a, t_d, t_p are the EV arrival, departure and parking time at workplace(h); SOC_a, B_a are the state of charge and energy stored in EV at arrival to work:

$$B_a = \frac{SOC_a}{100} B \qquad t_p = t_d - t_a \qquad (11a, b)$$

$$P = \frac{1000}{B_a t_p} \qquad (12)$$

The car with the highest priority is charged first. This method will give preference to EV with low energy and less parking time, to charge first. Thus 30 kW h of energy is delivered in total to the three cars and the excess PV is fed to the grid. If any of the cars require additional energy or if a fourth car D has to be charged, then charging region D is utilized, where the EV is charged partly from PV and partly from the grid.

5. Integrating local storage in EV–PV charger

Due to seasonal and diurnal variation in solar insolation, grid connection becomes pivotal and acts an energy buffer. Besides the grid, a local storage in the form of a battery bank can be used as well. In this section, the possibilities of using a local battery storage to eradicate the grid dependence of the EV–PV charger will be investigated.

At first, a 10 kW h lithium ion battery bank is integrated in the EV–PV charger. The battery is charged and discharged at a maximum C-rate of 1 C corresponding to a maximum charging/discharging power of P_b^{max} = 10 kW. The maximum depth of discharge is restricted to 80% (between state of charge (SOC) of 10–90%) to ensure long lifetime of the storage. Efficiency of

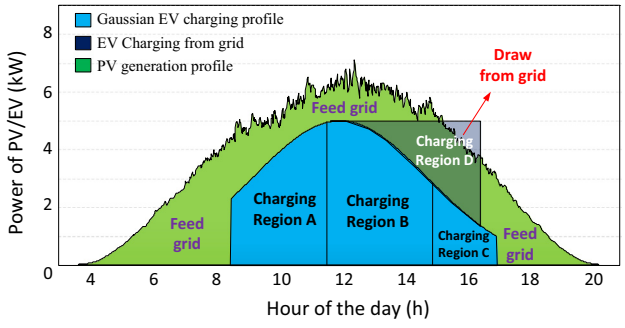

Fig. 12. Charging multiple EV using Gaussian charging profile.

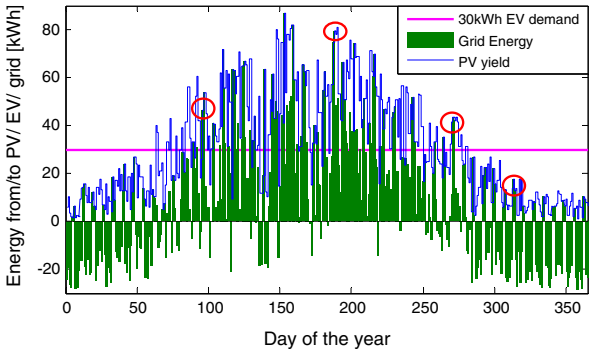

Fig. 13. Daily energy yield of PV and energy fed/drawn from grid for 30 kW h EV load profile G4 on weekdays.

charging/discharging of the battery including power converter is assumed to be 93% [57,58] and the efficiency of power exchange with the grid is considered as 95% [59].

Fig. 14 shows the state diagram for the operation of the EV–PV charger with local storage. Power is exchanged with the grid only when the storage is full/empty or if the maximum power limit of the storage is reached due to C-rate limitations. If there is a surplus of PV power above the EV demand, it is first used to charge the local storage, while a power deficit is first extracted from the local storage.

If the EV demand P_{EV} is more than the maximum charging/discharging power of the storage P_b^{max} due to C-rate limitations, then P_b^{max} is supplied to the EV from the storage and $|P_{EV} - P_b^{max}|$ is drawn from the grid to supply EV. The local storage never feeds/draws power from the grid; it interacts only with EV and PV.

Fig. 15 shows the power exchanged with the grid and the stored energy in local battery bank for 2013 (1 min resolution), considering EV loads for both 7 days/week and only on weekdays using profile G4. For 7 days/week load, it can be clearly observed that the battery is eternally empty in the winter months due to lack of excess PV power for charging it. Similarly the battery is full in the summer months (Day 80 to Day 270) due to high PV generation.

However, the local storage has a positive effect in the case of 5 days/week EV load. As seen in Fig. 15, the local storage gets periodically charged during the weekends even in winter (days 0–50 and days 300–365) as there is no EV and this helps supply the EV energy demands on Mondays and Tuesdays. However for the rest of the week, the storage is depleted of energy in winter and remains full in summer.

Since 10 kW h storage is insufficient for making the EV–PV charger grid independent, the storage size was varied from 5 kW h to 75 kW h to study its impact on the grid energy exchange, as shown in Figs. 16 and 17. It can be observed in Fig. 16 that the energy exchanged with the grid reduces with increasing storage size up to a certain point and then saturates henceforth. This means that even with large storage of up to 75 kW h, there is still a minimum amount of energy drawn/fed to the grid and it is not possible to make the EV–PV charger grid independent. This is especially true for a country like Netherlands which shows five times difference in summer and winter sunshine.

Storage SOC remaining >95% or <5% are both not good for the system as it leaves the battery in an unutilized state; it is either nearly empty or fully charged. Since the battery is used with DoD of 80%, SoC of 95% and 5% are scaled according to the 80% used capacity of the battery. Fig. 17 shows that increasing the storage size has minimal impact in improving the utilization of the battery. For a 5-day load profile, the battery is nearly full or empty (SOC >95% or <5%) for 70% of the time with 30 kW h storage and for

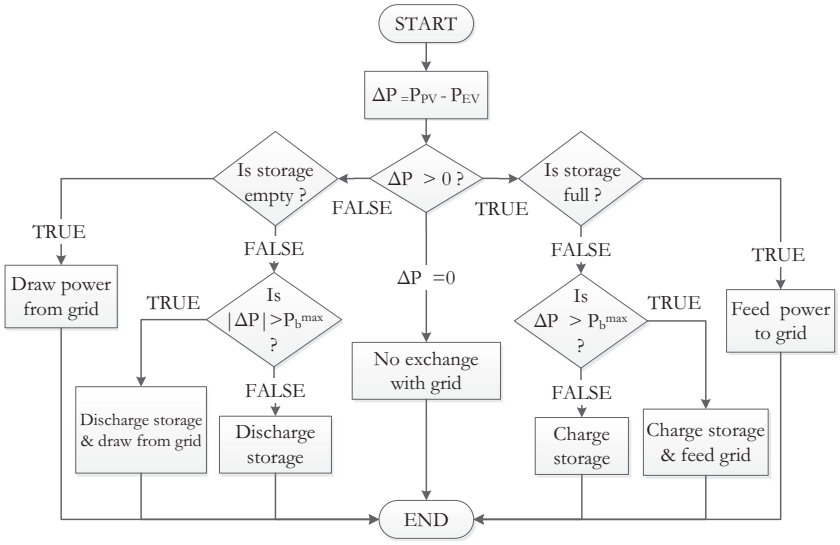

Fig. 14. State diagram for operation of EV–PV charger with local storage.

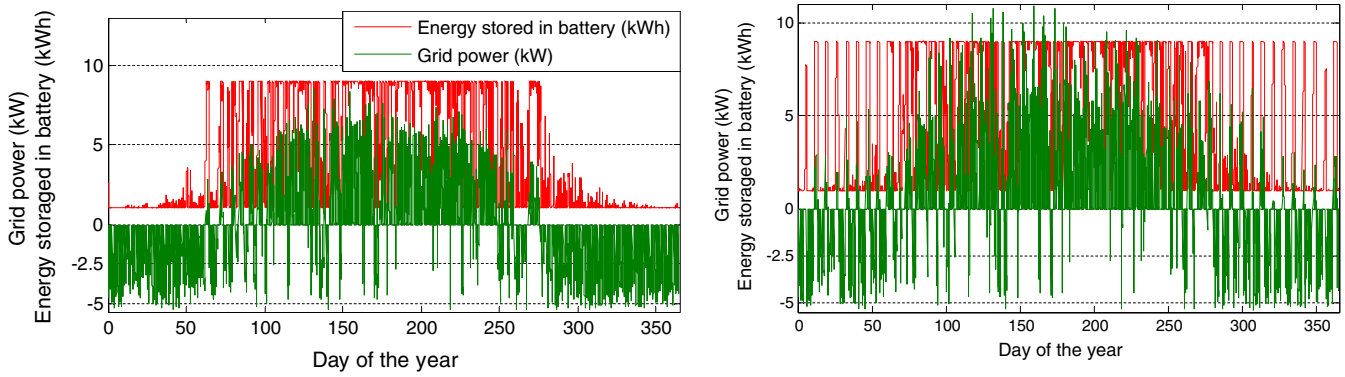

Fig. 15. Power exchanged with the grid (kW) and the stored energy in local storage (kW h) for the EV–PV charger for the year 2013 considering EV loads for 7 days/week (left) and only on weekdays (right).

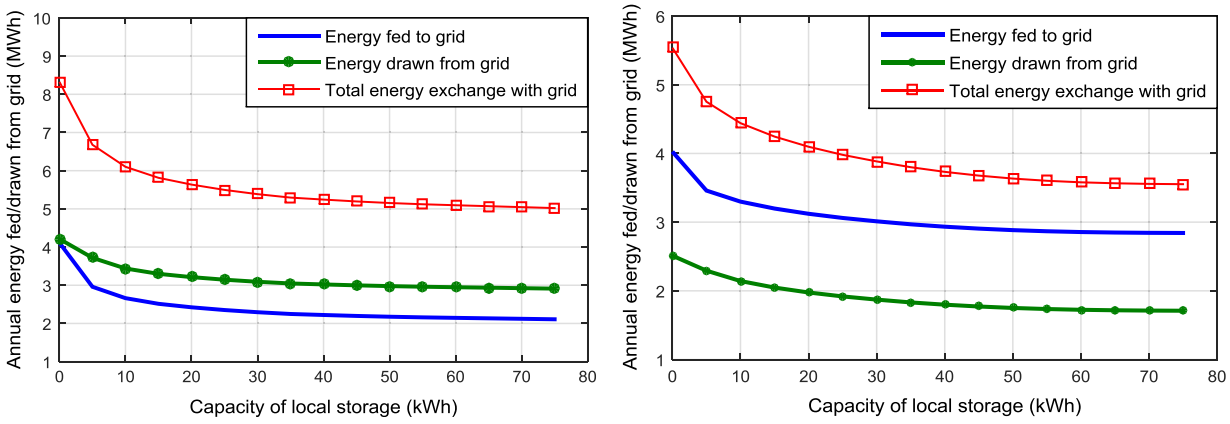

Fig. 16. Annual Energy exchanged with the grid for 2013 as a function of storage size, considering EV loads for 7 days/week (left) and only on weekdays (right) using Gaussian EV profile G4.

65% of the time with 75 kW h storage. This proves that with increasing the storage size by 2.5 times, the utilization of the battery is not proportional. Further the percentage of time in a year for which the EV–PV charger feeds/draws power from the grid does not reduce much with increasing storage size as seen in Fig. 17. In case of 5 day/week load, percentage of time for which energy is fed to grid is relatively much higher than for 7 day/week load and the percentage of time when energy is drawn from grid is lower.

From Fig. 16, it can be noted that small storage in the range of 5–15 kW h exhibits a drastic reduction in grid dependency. This is because 75% of variation in solar insolation between consecutive

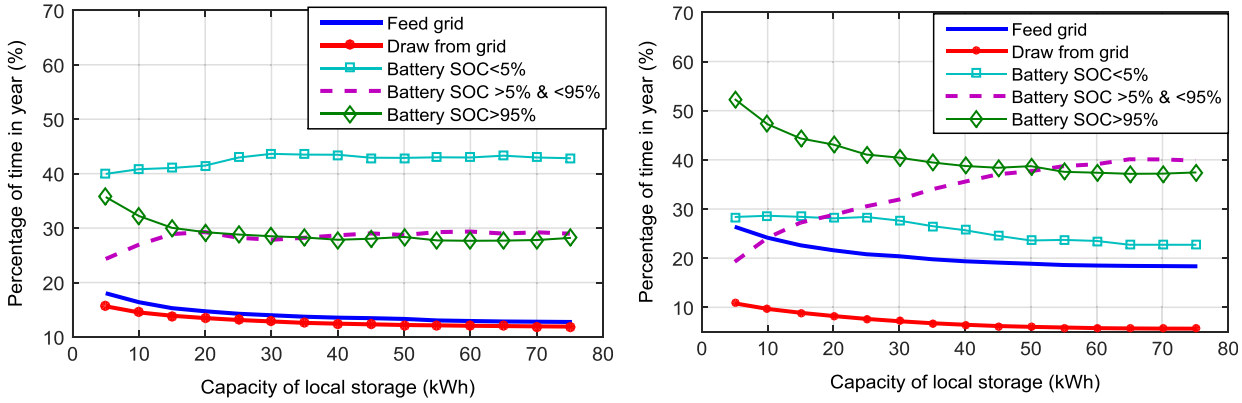

Fig. 17. Percentage of time in year when energy is exchanged with grid and battery exhibits specific state of charge for 7 days/week (left) and only on weekdays (right) using Gaussian EV profile G4.

days is less than 15 kW h. A small storage hence helps in balancing out diurnal and day–day solar variations. For 5 day/week and 7 days/week EV loads, the size of storage to achieve 25% reduction in energy exchanged with the grid is 10 kW h. A 10 kW h storage using Li-ion batteries will cost 8000–13,000 euros [60]. If a smaller storage is preferred, a 5 kW h storage can result in 17% and 20% reduction in grid energy exchange for 5 day/week and 7 day/week EV load respectively.

6. Conclusions

Workplace charging of EV from solar energy provides a sustainable gateway for transportation in the future. It provides a direct utilization of the PV power during the day and exploits the solar potential rooftops of buildings. In this paper, the PV system design and dynamic charging for a solar energy powered EV charging station for Netherlands is investigated.

Using data from KNMI, it was seen that the optimal tilt for PV panels in the Netherlands to get maximum yield is 28°. The annual yield of a 10 kW PV system using Sunpower modules was 10,890 kW h. Using a 2-axis solar tracker increases the yield by 17%, but this gain is concentrated in summer. Solar tracking was thus found to be ineffective in increasing the winter yield, which is the bottleneck of the system. The average daily PV energy production exhibits a difference of five times between summer and winter. This necessitates a grid connection for the EV–PV charger to supply power in winter and to absorb the excess PV power in summer.

Since high intensity insolation occurs rarely in the Netherlands, the PV power converter can be undersized with respect to the PV array by 30%, resulting in a loss of only 3.2% of the energy. Such a technique can be used for different metrological conditions in the world for optimally sizing the power converter with respect to the peak power array for the array.

Dynamic charging of EV facilitates the variation of EV charging power so as to closely follow the solar generation. Since solar generation exhibits a Gaussian variation with time over a 24 h period, Gaussian EV charging profile with a peak at 1200 h and a peak lesser than the installed peak power of the solar panels would be most ideal. The exact value of the Gaussian peak and width are location dependent. EV charging using Gaussian charging profile G3 and G4 with peak power of 5 kW and 4 kW were found to closely follow the PV generation curve of Netherlands. They delivered 30 kW h energy to the EV for both 5 days/week and 7 days/week EV load and resulted in minimum energy exchange with the grid. For charging multiple EV at workplace, a priority mechanism was proposed that will decide the order of precedence for EV charging, based on stored energy and parking time of EV.

It was proved that a local battery storage does not eliminate the grid dependence of the EV–PV charger in Netherlands, especially due to seasonal variations in insolation. However small sized storage in the order of 10 kW h helped in mitigating the day–day solar variations and reduced the grid energy exchange by 25%. The storage remains empty in winter for 7 days/week load and gets periodically full in weekends for 5 days/week load. The storage sizing is site specific and methodology presented here can be used for different locations to determine the optimal storage size.

Acknowledgements

The authors would like to sincerely thank and acknowledge the guidance and support of Assistant professor O.Isabella, PhD student V.Prasanth, V.Garita, N.Narayanan and researchers G.Nair, M.Leendertse from the Department of Electrical Sustainable Energy, Delft University of Technology; employees of Power Research Electronics B.V, Breda and ABB Product Group EV Charging Infrastructure, Rijswijk and the reviewers of the journal. This work was supported by TKI Switch2SmartGrids grant, Netherlands.

References

[1] Photovoltaic (PV) pricing trends: historical, recent, and near-term projections. National Renewable Energy Laboratory; 2012.
[2] Ministry of Transport Public Works and Water Management. Plan van Aanpak Elektrisch Rijden; 2011.
[3] Chandra Mouli GR, Bauer P, Wijekoon T, Panosyan A, Barthlein E-M. Design of a power-electronic-assisted OLTC for grid voltage regulation. IEEE Trans Power Delivery 2015;30:1086–95. http://dx.doi.org/10.1109/TPWRD.2014.2371153.
[4] Singh M, Thirugnanam K, Kumar P, Kar I. Real-time coordination of electric vehicles to support the grid at the distribution substation level. IEEE Syst J 2015;9:1000–10. http://dx.doi.org/10.1109/JSYST.2013.2280821.
[5] Thirugnanam K, Ezhil Reena JTP, Singh M, Kumar P. Mathematical modeling of Li-ion battery using genetic algorithm approach for V2G applications. IEEE Trans Energy Convers 2014;29:332–43. http://dx.doi.org/10.1109/TEC.2014.2298460.
[6] Das R, Thirugnanam K, Kumar P, Lavudiya R, Singh M. Mathematical modeling for economic evaluation of electric vehicle to smart grid interaction. IEEE Trans Smart Grid 2014;5:712–21. http://dx.doi.org/10.1109/TSG.2013.2275979.
[7] Thirugnanam K, Joy TPER, Singh M, Kumar P. Modeling and control of contactless based smart charging station in V2G scenario. IEEE Trans Smart Grid 2014;5:337–48. http://dx.doi.org/10.1109/TSG.2013.2272798.
[8] Solar electric vehicle charging station. University of Iowa; n.d. <http://facilities.uiowa.edu/uem/renewable-energy/solar-energy.html>.
[9] Choe G-Y, Kim J-S, Lee B-K. A Bi-directional battery charger for electric vehicles using photovoltaic PCS systems. In: 2010 IEEE veh power propuls conf, IEEE; 2010. p. 1–6. http://dx.doi.org/10.1109/VPPC.2010.5729223.
[10] Hamilton C, Gamboa G, Elmes J, Kerley R, Arias A, Pepper M, et al. System architecture of a modular direct-DC PV charging station for plug-in electric vehicles. In: IECON 2010 – 36th annu conf IEEE ind electron soc, IEEE; 2010. p. 2516–20. http://dx.doi.org/10.1109/IECON.2010.5675158.

[11] Noriega BE, Pinto RT, Bauer P. Sustainable DC-microgrid control system for electric-vehicle charging stations. In: 2013 15th Eur conf power electron appl, IEEE; 2013. p. 1–10. http://dx.doi.org/10.1109/EPE.2013.6634620.

[12] Chandra Mouli GR, Bauer P, Zeman M. Comparison of system architecture and converter topology for a solar powered electric vehicle charging station. In: 9th Int. Conf. Power Electron. ECCE Asia (ICPE-ECCE Asia), IEEE; 2015. p. 1908–15. http://dx.doi.org/10.1109/ICPE.2015.7168039.

[13] Laboratory Oak Ridge National. Solar-assisted electric vehicle charging stations; 2011.

[14] Goli P, Shireen W. PV powered smart charging station for PHEVs. Renew Energy 2014;66:280–7. http://dx.doi.org/10.1016/j.renene.2013.11.066.

[15] Gamboa G, Hamilton C, Kerley R, Elmes S, Arias A, Shen J, et al. Control strategy of a multi-port, grid connected, direct-DC PV charging station for plug-in electric vehicles. In: 2010 IEEE energy convers congr expo, IEEE; 2010. p. 1173–7. http://dx.doi.org/10.1109/ECCE.2010.5617838.

[16] Fattori F, Anglani N, Muliere G. Combining photovoltaic energy with electric vehicles, smart charging and vehicle-to-grid. Sol Energy 2014;110:438–51. http://dx.doi.org/10.1016/j.solener.2014.09.034.

[17] Capasso C, Veneri O. Experimental study of a DC charging station for full electric and plug in hybrid vehicles. Appl Energy 2015;152:131–42. http://dx.doi.org/10.1016/j.apenergy.2015.04.040.

[18] Denholm P, Kuss M, Margolis RM. Co-benefits of large scale plug-in hybrid electric vehicle and solar PV deployment. J Power Sources n.d.

[19] Birnie DP. Solar-to-vehicle (S2V) systems for powering commuters of the future. J Power Sources 2009;186:539–42. http://dx.doi.org/10.1016/j.jpowsour.2008.09.118.

[20] Nunes P, Farias T, Brito MC. Day charging electric vehicles with excess solar electricity for a sustainable energy system. Energy 2015;80:263–74. http://dx.doi.org/10.1016/j.energy.2014.11.069.

[21] Tulpule PJ, Marano V, Yurkovich S, Rizzoni G. Economic and environmental impacts of a PV powered workplace parking garage charging station. Appl Energy 2013;108:323–32. http://dx.doi.org/10.1016/j.apenergy.2013.02.068.

[22] Tulpule P, Marano V, Yurkovich S, Rizzoni G. Energy economic analysis of PV based charging station at workplace parking garage. In: IEEE 2011 EnergyTech, IEEE; 2011. p. 1–6. http://dx.doi.org/10.1109/EnergyTech.2011.5948504.

[23] van der Kam M, van Sark W. Smart charging of electric vehicles with photovoltaic power and vehicle-to-grid technology in a microgrid; a case study. Appl Energy 2015;152:20–30. http://dx.doi.org/10.1016/j.apenergy.2015.04.092.

[24] Nunes P, Farias T, Brito MC. Enabling solar electricity with electric vehicles smart charging. Energy 2015;87:10–20. http://dx.doi.org/10.1016/j.energy.2015.04.044.

[25] Cutler SA, Schmalberger B, Rivers C. An intelligent solar ecosystem with electric vehicles. In: 2012 IEEE int electr veh conf, IEEE; 2012. p. 1–7. http://dx.doi.org/10.1109/IEVC.2012.6183168.

[26] Mesentean S, Feucht W, Kula H-G, Frank H. Smart charging of electric scooters for home to work and home to education transports from grid connected photovoltaic-systems. In: 2010 IEEE int energy conf, IEEE; 2010. p. 73–8. http://dx.doi.org/10.1109/ENERGYCON.2010.5771778.

[27] Kadar P, Varga A. PhotoVoltaic EV charge station. In: 2013 IEEE 11th int symp appl mach intell informatics, IEEE; 2013. p. 57–60. http://dx.doi.org/10.1109/SAMI.2013.6480944.

[28] Brenna M, Dolara A, Foiadelli F, Leva S, Longo M. Urban scale photovoltaic charging stations for electric vehicles. IEEE Trans Sustain Energy 2014;5:1234–41. http://dx.doi.org/10.1109/TSTE.2014.2341954.

[29] Dziadek P-E, Feucht W, Mittnacht A, Kula H-G, Frank H. Eco-friendly application of EVs for home-to-work and home-to-education transports. In: 2013 IEEE int conf ind technol, IEEE; 2013. p. 705–9. http://dx.doi.org/10.1109/ICIT.2013.6505758.

[30] Mesentean S, Feucht W, Mittnacht A, Frank H. Scheduling methods for smart charging of electric bikes from a grid-connected photovoltaic-system. In: 2011 UKSim 5th Eur symp comput model simul, IEEE; 2011. p. 299–304. http://dx.doi.org/10.1109/EMS.2011.88.

[31] Kawamura N, Muta M. Development of solar charging system for plug-in hybrid electric vehicles and electric vehicles. In: 2012 Int conf renew energy res appl, IEEE; 2012. p. 1–5. http://dx.doi.org/10.1109/ICRERA.2012.6477383.

[32] Gurkaynak Y, Khaligh A. Control and power management of a grid connected residential photovoltaic system with plug-in hybrid electric vehicle (PHEV) load. In: 2009 Twenty-fourth annu IEEE appl power electron conf expo, IEEE; 2009. p. 2086–91. http://dx.doi.org/10.1109/APEC.2009.4802962.

[33] Gurkaynak Y, Khaligh A. A novel grid-tied, solar powered residential home with plug-in hybrid electric vehicle (PHEV) loads. In: 2009 IEEE veh power propuls conf, IEEE; 2009. p. 813–6. http://dx.doi.org/10.1109/VPPC.2009.5289765.

[34] Robalino DM, Kumar G, Uzoechi LO, Chukwu UC, Mahajan SM. Design of a docking station for solar charged electric and fuel cell vehicles. In: 2009 Int conf clean electr power, IEEE; 2009. p. 655–60. http://dx.doi.org/10.1109/ICCEP.2009.5211977.

[35] Tesfaye M, Castello CC. Minimization of impact from electric vehicle supply equipment to the electric grid using a dynamically controlled battery bank for peak load shaving. In: 2013 IEEE PES innov smart grid technol conf, IEEE; 2013. p. 1–6. http://dx.doi.org/10.1109/ISGT.2013.6497815.

[36] Castello CC, LaClair TJ, Maxey LC. Control strategies for electric vehicle (EV) charging using renewables and local storage. In: 2014 IEEE transp electrif conf expo, IEEE; 2014. p. 1–7. http://dx.doi.org/10.1109/ITEC.2014.6861835.

[37] SAE Standard J1772. SAE electric vehicle and plug-in hybrid electric vehicle conductive charge coupler; 2010.

[38] Standard IEC 62196 – plugs, socket-outlets, vehicle connectors and vehicle inlets – conductive charging of electric vehicles – Part 1, 2, 3; 2014.

[39] Bauer P, Yi Zhou, Doppler J, Stembridge N, Zhou Y. Charging of electric vehicles and impact on the grid. In: Proc 13th int symp mechatronics, mechatronika 2010; 2010. p. 121–7.

[40] Mackay L, Hailu TG, Chandra Mouli GR, Ramırez-Elizondo L, Ferreira JA, Bauer P. From DC nano- and microgrids towards the universal DC distribution system – a plea to think further into the future. In: 2015 IEEE power energy soc gen meet, IEEE; 2015. p. 1–5. http://dx.doi.org/10.1109/PESGM.2015.7286469.

[41] Marafante E, Mackay L, Hailu TG, Mouli GRC, Ramirez-Elizondo L, Bauer P. PV architectures for DC microgrids using buck or boost exclusive microconverters. In: 2015 IEEE Eindhoven PowerTech, IEEE; 2015. p. 1–6. http://dx.doi.org/10.1109/PTC.2015.7232733.

[42] CESAR Database. Koninklijk Nederlands Meteorologisch Instituut (KNMI); 2014. <http://www.cesar-Database.nl>.

[43] Datasheet, Sun power E20-327 PV module; 2015. <Http://global.sunpower.com/>.

[44] Approximate solar coordinates. The United States Naval Observatory (USNO); n.d. <http://aa.usno.navy.mil/faq/docs/SunApprox.php>.

[45] Michalsky JJ. The Astronomical Almanac's algorithm for approximate solar position (1950–2050). Sol Energy 1988;40:227–35. http://dx.doi.org/10.1016/0038-092X(88)90045-X.

[46] Loutzenhiser PPG, Manz H, Felsmann C, Strachan PA, Frank T, Maxwell GM. Empirical validation of models to compute solar irradiance on inclined surfaces for building energy simulation. Sol Energy 2007;81:254–67. http://dx.doi.org/10.1016/j.solener.2006.03.009.

[47] Sproul AB. Derivation of the solar geometric relationships using vector analysis. Renew Energy 2007;32:1187–205. http://dx.doi.org/10.1016/j.renene.2006.05.001.

[48] Ashok VV, Onwudinanti C, Chandra Mouli GR, Bauer P. Matching PV array output with residential and office load by optimization of array orientation. In: PowerTech (POWERTECH), 2015 IEEE Eindhoven, Eindhoven; 2015. http://dx.doi.org/10.1109/PTC.2015.7232610.

[49] Klucher TM. Evaluation of models to predict insolation on tilted surfaces. Sol Energy 1979;23:111–4. http://dx.doi.org/10.1016/0038-092X(79)90110-5.

[50] Skoplaki E, Palyvos JA. On the temperature dependence of photovoltaic module electrical performance: a review of efficiency/power correlations. Sol Energy 2009;83:614–24.

[51] Jakhrani AQ, Othman AK, Rigit ARH, Samo S. Comparison of solar photovoltaic module temperature models. World Appl Sci J 2011.

[52] Isabella O, Nair GG, Tozzi A, Castro Barreto JH, Chandra Mouli GR, Lantsheer F, et al. Comprehensive modelling and sizing of PV systems from location to load. MRS Proc 2015;1771. http://dx.doi.org/10.1557/opl.2015.347. mrss15-2138558.

[53] Drury E, Lopez A, Denholm P, Margolis R. Relative performance of tracking versus fixed tilt photovoltaic systems in the USA. Prog Photovoltaics Res Appl 2013. http://dx.doi.org/10.1002/pip.237.

[54] Hocaoglu FO, Gerek ÖN, Kurban M. Solar radiation data modeling with a novel surface fitting approach. In: Ishikawa M, Doya K, Miyamoto H, Yamakawa T, editors. Neural inf process, vol. 4985. Berlin, Heidelberg: Springer; 2008. p. 460–7. http://dx.doi.org/10.1007/978-3-540-69162-4.

[55] Hocaoglu FO, Gerek ON, Kurban M. The effect of model generated solar radiation data usage in hybrid (wind–PV) sizing studies. Energy Convers Manage 2009;50:2956–63. http://dx.doi.org/10.1016/j.enconman.2009.07.011.

[56] Harikumaran J, Vereczki G, Farkas C, Bauer P. Comparison of quick charge technologies for electric vehicle introduction in Netherlands. In: IECON proc industrial electron conf, IEEE; 2012. p. 2907–13. http://dx.doi.org/10.1109/IECON.2012.6389433.

[57] Specifications – Tesla Powerwall (7 kW h, 350–450V); 2015. <https://www.teslamotors.com/powerwall>.

[58] Lam L, Bauer P. Practical capacity fading model for Li-ion battery cells in electric vehicles. IEEE Trans Power Electron 2013;28:5910–8. http://dx.doi.org/10.1109/TPEL.2012.2235083.

[59] SMA. Datasheet – SMA SUNNY ISLAND 6.0H/8.0H; 2015.

[60] Dufo-López R, Bernal-Agustín JL. Advances in mechanical and electronic engineering. Berlin, Heidelberg: Springer; 2013. http://dx.doi.org/10.1007/978-3-642-31528-2. vol. 178.